

# Stroke-Based Scene Text Erasing Using Synthetic Data

Zhengmi Tang, Tomo Miyazaki, *Member, IEEE*, Yoshihiro Sugaya, *Member, IEEE*, and Shinichiro Omachi, *Senior Member, IEEE*

**Abstract**—Scene text erasing, which replaces text regions with reasonable content in natural images, has drawn attention in the computer vision community in recent years. There are two potential subtasks in scene text erasing: text detection and image inpainting. Either sub-task requires considerable data to achieve better performance; however, the lack of a large-scale real-world scene-text removal dataset allows the existing methods to not work in full strength. To avoid the limitation of the lack of pairwise real-world data, we enhance and make full use of the synthetic text and consequently train our model only on the dataset generated by the improved synthetic text engine. Our proposed network contains a stroke mask prediction module and background inpainting module that can extract the text stroke as a relatively small hole from the text image patch to maintain more background content for better inpainting results. This model can partially erase text instances in a scene image with a bounding box provided or work with an existing scene text detector for automatic scene text erasing. The experimental results of qualitative evaluation and quantitative evaluation on the SCUT-Syn, ICDAR2013, and SCUT-EnsText datasets demonstrate that our method significantly outperforms existing state-of-the-art methods even when trained on real-world data.

**Index Terms**—Scene text erasing, Synthetic text, Background inpainting

## I. INTRODUCTION

TEXTS created by humankind carry rich, precise high-level semantics, and text around us in our daily life provides us with a considerable amount of valuable information. However, with the increasing population of portable devices, such as digital cameras, tablets, smartphones and SNS, a huge amount of scene images, including text, are published on the internet every second, and these texts could contain private information such as names, addresses, and vehicle number plates. With the increasing development of scene text detection and recognition technology, there is a high risk that information is automatically collected and used for illegal purposes. Therefore, scene text erasing, which is replacing text regions in scene images with proper content has drawn attention in the computer vision community in recent years.

After the prior work of Scene Text Eraser [1], scene text erasing research has developed into two directions: one-step and two-step methods. [2]–[4] are the representative works of one-step methods combining the text detection and inpainting functions into one network, which makes one-step method



Fig. 1. Scene Text Erasing: original images and text bounding boxes (left); text-erased images by our method (middle); predicted text stroke mask (right).

light-weight and fast, and does not need input any text location information. The drawback is that the text localization mechanism of these networks is weak, and the text-erasing process is not controllable. To allow for the network to learn the complicated distribution of scene texts, a considerable number of manual text-erased real-world images are required as training data because the text distribution of the Synth-text [5] dataset, which is generated according to human rules, is significantly different from the real-world one. To generate scene-text-erased images [4], [6], photo editing software such as Photoshop is used to fill the text region with visually plausible content in natural images. However, this type of annotation is expensive and time-consuming because the annotators need to operate carefully to guarantee the erasing quality, especially when facing a text instance on a complicated background. The two-step approaches decompose the text-erasing task into two sub-problems: text detection and background inpainting. Zdenek *et al.* [7] used a pretrained scene text detection model and inpainting model to erase the text in the wild as a weak supervision method, which does not require paired training data. However, the inpainting model is trained in the Street View [8] or ImageNet [9] datasets; thus, the pretrained models face domain shift problems, which cannot fit perfectly in the context of scene text.

In this study, we propose a scene-text-erasing network that works on the text image patch level. It follows: first predict the text stroke as a hole, then inpaint it, and train it in an end-to-end fashion. To avoid the limitation of the lack of pairwise real-world data and make full use of the appearance of synthetic texts, we improve the appearance effect of synthetic

Manuscript received March 10, 2021. This work was partially supported by JSPS KAKENHI Grant Numbers 18K19772, 19K12033, 20H04201.

The authors are with the Graduate School of Engineering, Tohoku University, Sendai, 980-8579, Japan. (e-mail: tzm@dc.tohoku.ac.jp, tomo@tohoku.ac.jp, sugaya@iic.ecei.tohoku.ac.jp, machi@ecei.tohoku.ac.jp).

text [5] and train our model only on the dataset generated by the improved synthetic text engine. This model can partially erase text instances in a scene image if text bounding boxes are provided or work with existing scene text detectors for automatic scene text erasing. Examples of text-erasing results obtained by our proposed method are shown in Fig. 1.

In summary, the main contributions of our study are summarized as follow:

- We propose a stroke-based text-erasing network, which contains the Stroke Mask Prediction Module and the Background Inpainting Module. Benefiting from the network structure, our method could erase the text region while retaining more background information along with texture restoration.
- We enhance Text Synthesis Engine [5] to make the appearance of synthetic text instances share more similarity with real-world data.
- The quantitative and qualitative evaluation results on SCUT-Syn [3], ICDAR 2013 [10] and SCUT-EnsText [4] datasets show that our method outperforms previous state-of-the-art methods while it is only trained on the dataset generated by the improved synthetic text engine [5].

The remainder of this paper is structured as follows. Section II reviews related works on scene text detection, image inpainting, and text erasing. Section III introduces the details of our method, including the pipeline and the proposed networks. In Section IV, our proposed method is evaluated and compared with related inpainting and scene text erasing studies through experiments. Finally, we provide concluding statements in Section V.

## II. RELATED WORK

### A. Scene Text Detection

The emergence of deep learning has facilitated the development of scene text detection research and shows promising performance compared to traditional manually designed algorithms [11]–[15]. Recent learning-based scene text detection methods have been inspired by general object detection and image segmentation methods. TextBoxes [16] adjusted the aspect ratios of anchors in SSD [17] to detect text with different shapes. CTPN [18] combined the framework of Faster R-CNN [19] with a recurrence mechanism to predict the contextual and dense components of text. RRPN [20] proposed a rotation region proposal to bind multi-oriented scene text with rotated rectangles. SegLink [21] predicted text segments and their links and combined them into the final detection. EAST [22] directly regresses rotated rectangles or quadrangles of text through a simplified pipeline without using any anchors. In recent years, curved text [23] has attracted the interest of the research community because rectangular or quadrilateral annotations loosely bound curved text. Mask textspotter [24] built a model based on the framework of Mask R-CNN [25] and performed character-level instance segmentation for each alphabet. TextSnake [26] proposed a novel representation of arbitrarily shaped text and predicted heat maps of text center lines, text regions, radii, and orientations to extract text regions. CRAFT [27] proposed learning each character

center and affinity between characters in the form of a heat map. PSENet [28] gradually expands the text region from small kernels to large ones and makes final predictions through multiple semantic segmentation maps.

### B. Image Inpainting

Image inpainting fills the hole regions of an images with plausible content. Image inpainting researches can generally be divided into two categories: non-learning approaches and deep-learning-based approaches. Non-learning approaches transfer surrounding contents to the hole regions based on low-level features using a traditional algorithm such as patch matching [29]–[32]. Although those methods can work well on small holes, they cannot deal with large missing regions, where semantics patch should be selected for the hole restoration based on a high-level understanding of the whole image.

Deep-learning-based approaches, especially the generative adversarial network (GAN) strategy, have been widely adopted in recent image inpainting research. Context encoders [8] first trained an image inpainting deep neural networks using an encoder-decoder structure and adversarial losses. To generate a more realistic texture, the coarse-to-fine strategy was adopted. Iizuka *et al.* [33] adopted dilated convolution and proposed global and local discriminators for adversarial training. Liu *et al.* [34] defined a partial convolutional layer with a mask-update mechanism to ensure that the partial convolution filters learn more valid information from the non-hole region and can robustly handle holes of any shape. Yu *et al.* [35] further proposed gate convolution that makes the mask-update mechanism learnable and combines it with the SN-PatchGAN discriminator to obtain better performance. Xie *et al.* [36] proposed a learnable bidirectional attention module that included forward and reverse attention maps for more effective hole filling. Li *et al.* [37] exploited the correlation between adjacent pixels by recurrently inferring and gathering the hole boundary for the encoder, named the recurrent feature reasoning module. Yi *et al.* [38] proposed a contextual residual aggregation mechanism that enables more efficient and high-quality ultra-high-resolution image inpainting.

### C. Text Erasing

Early text erasing research starts with the removal of born-digital text such as watermarks, captions, and subtitles on images or video sequences [39]. Owing to the plain layout, color, and regular font, born-digital text can be detected by traditional feature engineering approaches, such as binarization [40], [41], and inpainted by patch matching [42] or smoothing algorithm [43].

Erasing text in the wild is a more complex and challenging task owing to its various fonts with different layouts and illumination conditions. The recent rapid development of deep neural networks has made scene text erasing a promising research task in the computer vision field. Nakamura *et al.* [1] made the first attempt to build a one-stage scene text eraser—a sliding window method using a U-Net structure convolutional neural network. It destroys the integrity of text strokes but cannot maintain the global consistency of the entire image.

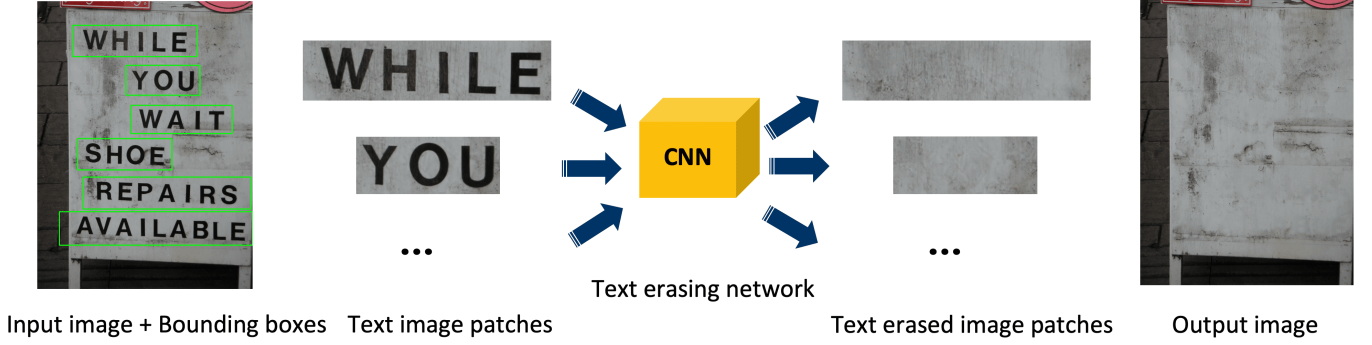


Fig. 2. Pipeline of our proposed method.

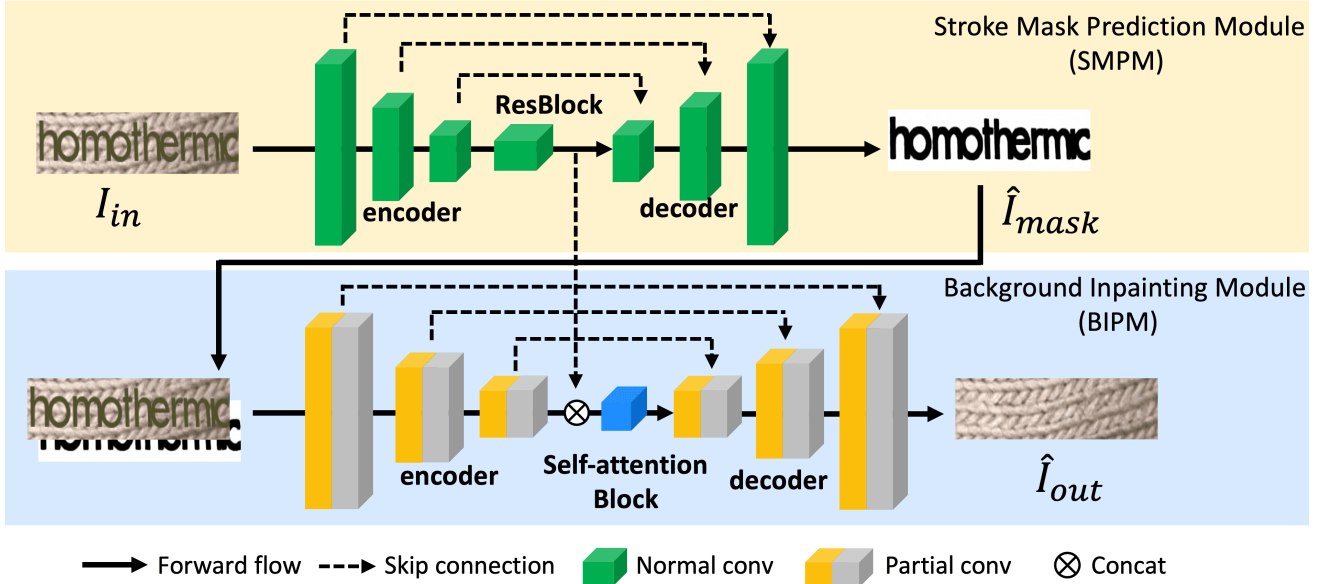


Fig. 3. Structure of our proposed network. It is composed of a stroke mask prediction module (SMPM) (top) and the background inpainting module (BIPM)(bottom)

Recent studies have focused on the entire image level based on GANs. EnsNet [3] adopts conditional generative adversarial networks (cGAN) with a refined loss function and local-aware discriminator. MTRNet [44] uses text masks to guide the training and prediction processes of cGAN, thereby also realizing the controllability of the text-erasing region. Zdenek *et al.* [7] proposed a weak supervision method employing a pretrained scene text detector [28] and image inpainting model [45] that do not require paired-wise training data of scene images with text and their corresponding text-erased images. Liu *et al.* [4] provided a comprehensive real-world scene-text removal benchmark, named SCUT-EnsText, and proposed EraseNet adopting a coarse-to-fine erasure network structure with a segmentation head, which can generate a mask of the text region to help with text region localization. MTRNet++ [2] shares the same coarse-to-fine inpainting idea but uses a multi-branch generator. The mask-refine branch could predict stroke-level text masks to guide text removal. Partial text removal is also possible if a coarse mask is provided.

### III. METHODOLOGY

The pipeline of the proposed method is shown in Fig. 2. Given the input image and the text bounding boxes, text image patches are detected from the source image. Subsequently, each image patch goes through the text-erasing network, and we can obtain text-erased image patches. Putting these patches back to the source image, we can obtain the output images that do not contain text.

Our network comprises 1) a stroke mask prediction module and 2) a background inpainting module as illustrated in Fig. 3. Specifically, the stroke mask prediction module first predicts the stroke mask of scene text  $\hat{I}_{mask}$  as the hole from  $I_{in}$ . Then, the background inpainting module is used to fill the hole of the input image  $I_{in}$  with the appropriate content and output text-erased image  $\hat{I}_{out}$ .

#### A. Stroke Mask Prediction Module

An encoder-decoder FCN was adopted in this module. The input image patch  $I_{in}$  is encoded by three downsampling

convolutional layers and four residual blocks [46], and the feature maps  $F_m$  are decoded by three upsampling transposed convolutional layers to generate the text stroke mask  $\hat{I}_{mask}$ . The skip connections concatenate feature maps with the same shape between the encoder and the decoder. The feature maps  $F_m$  output from the residual blocks are concatenated with the feature maps  $F_b$  in the background inpainting module, which will be introduced later. The dice loss [47] and L1 loss were used to guide the generation of the text mask. Mathematically, the dice loss is defined as

$$\mathcal{L}_{dice} = 1 - \frac{2 \sum_i^N (\hat{I}_{mask})_i (I_{mask})_i}{\sum_i^N (\hat{I}_{mask})_i + \sum_i^N (I_{mask})_i}, \quad (1)$$

where  $N$  denotes the total number of pixels in the input image, and  $\hat{I}_{mask}$  and  $I_{mask}$  represent the prediction and ground truth of a text mask, respectively. The total loss of the stroke mask prediction module is

$$\mathcal{L}_{SMPM} = \|\hat{I}_{mask} - I_{mask}\|_1 + \lambda_0 \mathcal{L}_{dice}, \quad (2)$$

and in our experiments,  $\lambda_0$  is set to 1.0.

### B. Background Inpainting Module

In this module, the input image  $I_{in}$  and the predicted mask image  $\hat{I}_{mask}$  are taken as its input, and it outputs a background image  $O_b$ , in which all text stroke pixels, including text shadows caused by illumination, are replaced with proper texture. As shown in the blue part of Fig. 3, the input image is encoded by three downsampling partial convolutional layers and concatenated with the feature map  $F_m$  from the stroke mask prediction module. A self-attention block follows and lets the network learn long-range dependencies. Finally, the decoder generates the output image  $\hat{I}_{out}$ .

1) *Partial Convolutional Layers*: To generate clearer background images and suppress text ghosts and artifacts, we use partial convolutional layers [34] to allow the network to learn more features from the non-text part of  $I_{in}$ . The partial convolution layer comprises two steps: partial convolution operation and mask update. Partial convolution operation and mask update are defined as follows:

$$x' = \begin{cases} \mathbf{W}^T(\mathbf{X} \odot \mathbf{M}) \frac{\text{sum}(\mathbf{1})}{\text{sum}(\mathbf{M})} + b, & \text{if } \text{sum}(\mathbf{M}) > 0 \\ 0, & \text{otherwise} \end{cases}, \quad (3)$$

$$m' = \begin{cases} 1, & \text{if } \text{sum}(\mathbf{M}) > 0 \\ 0, & \text{otherwise} \end{cases}, \quad (4)$$

where  $\mathbf{W}$  and  $b$  indicate the weights and bias of the convolution filter, respectively.  $\mathbf{X}$  are the input pixels for the current convolution window, and  $\mathbf{M}$  is the corresponding mask.  $\odot$  denotes element-wise multiplication.  $\mathbf{1}$  is an all-one matrix with the same shape as  $\mathbf{M}$ .

2) *Self-Attention Block*: Considering the feature maps  $F_m$  generated in the stroke mask prediction module contain feature information of texture and illumination effect inside the text region, after the concatenation of the feature maps  $F_m$  and  $F_b$  from the two modules, we fed concatenated feature maps to a self-attention network that learns both the correspondences between feature maps and non-local features. We adopt a

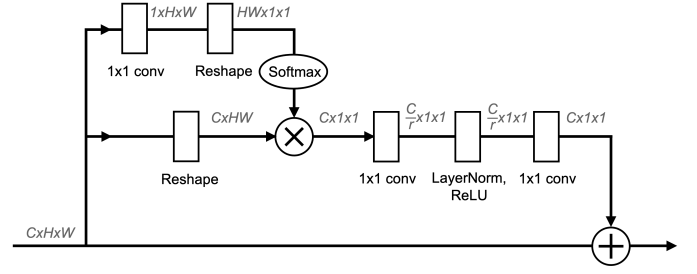


Fig. 4. Architecture of self-attention block: Global Context (GC) block.

global context (GC) block [48], and the architecture of a GCblock is depicted in Fig. 4.

The loss function of the background inpainting module includes four parts shown as below:

$$\mathcal{L}_{BIPM} = \mathcal{L}_{pixel} + \lambda_1 \mathcal{L}_{per} + \lambda_2 \mathcal{L}_{style} + \lambda_3 \mathcal{L}_{tv}, \quad (5)$$

where,  $\lambda_1$ ,  $\lambda_2$ , and  $\lambda_3$  are set to 0.05, 150, and 0.1, respectively.

Pixel loss targets the guiding pixel-level reconstruction, which adds more weight to the hole region.

$$\mathcal{L}_{pixel} = \|\hat{I}_{mask} \odot (\hat{I}_{out} - I_{out})\|_1 + 6\|(1 - \hat{I}_{mask}) \odot (\hat{I}_{out} - I_{out})\|_1. \quad (6)$$

Perceptual loss and style loss, which is also known as VGG loss [49], [50] are used to make the generated image more realistic.

$$\mathcal{L}_{per} = \mathbb{E}[\sum_{i=1} \|\phi_i(\hat{I}_{out}) - \phi_i(I_{out})\|_1 + \sum_{i=1} \|\phi_i(I_{comp}) - \phi_i(I_{out})\|_1], \quad (7)$$

$$\mathcal{L}_{style} = \mathbb{E}_j[\|G_j^\phi(\hat{I}_{out}) - G_j^\phi(I_{out})\|_1 + \|G_j^\phi(I_{comp}) - G_j^\phi(I_{out})\|_1], \quad (8)$$

where  $\phi_i$  is the activation map from the relu1\_1 to the relu5\_1 layer of a pretrained VGG-16 model.  $G$  is a gram matrix. and  $I_{comp}$  are defined as follows:

$$I_{comp} = \hat{I}_{mask} \odot I_{out} + (1 - \hat{I}_{mask}) \odot \hat{I}_{out}. \quad (9)$$

Total variation loss is employed to maintain spatial continuity and smoothness in the generated image to reduce the effect of noise.

$$\mathcal{L}_{tv} = \sum_{(i,j,j+1) \in M} \|I_{comp}^{i,j+1} - I_{comp}^{i,j}\|_1 + \sum_{(i,j,i+1) \in M} \|I_{comp}^{i+1,j} - I_{comp}^{i,j}\|_1, \quad (10)$$

where  $M$  is the hole region in  $\hat{I}_{mask}$ .

Finally, the loss function of the whole network is:

$$\mathcal{L} = \mathcal{L}_{SMPM} + \mathcal{L}_{BIPM}. \quad (11)$$





Fig. 5. Some training image samples generated by our enhanced synthesis text engine. Input (top), final ground-truth (middle), text mask ground-truth (bottom)

#### IV. EXPERIMENT

##### A. Implementation Details

Our implementation is based on PyTorch. In the training process, we generated one million synthetic text images and corresponding text mask image patches as training data from the background images. The height of the input images was resized to 128 while maintaining the aspect ratio. The maximum width was 640. If the width of the image patch was insufficient, the remaining pixels were padded with 0. The batch size was eight on a single 1080Ti GPU. We used Adam [51] to optimize the entire network with  $\beta = (0.9, 0.999)$  and set the weight decay to 0. The learning rate started from 0.0002 and decayed to nine-tenth after each epoch in the training phase. The network was trained in an end-to-end manner, and we followed the fine-tune strategy [34], which freezes the batch normalization parameters in the encoder of the background inpainting module after approximately 10 epochs.

In the prediction process, we first expanded and cut the text bounding box to include more background information. Subsequently, we fed the expanded text image patch to our proposed network for prediction. Finally, part of the output, which is inside the original bounding box, is pasted back to the source image. The text in arbitrary quadrilateral annotation was transformed by perspective transformation, and text in curved annotation was transformed by thin-plate-spline into rectangular text images before feeding them into our network. The network output is transformed back to its original shape and copied to the original position to obtain the final text-erased image.

##### B. Dataset and Evaluation Metrics

###### 1) Synthetic Dataset:

- **Improved Synth-text image patches** We used over 1,500 English and Chinese fonts and 10,000 background images without text to generate a total of one million image patches for our model training using our enhanced synthesis text engine, which is improved from Synth-text technology [5]. The training dataset contains original background images as the final ground truth, synthetic text in background images as input, and mask images of synthetic text as the ground truth of the text mask. Compared with the vanilla synth-text method, we made several improvements to make our generated data share

more similarity with real-world data. 1) There is a 50% possibility that the text instance will be composed directly on the background instead of using only Poisson blending because Poisson blending would provide some background information behind the text instance. 2) Some other effects were added to the text instance, such as Gaussian blur to simulate out of focus, text shift to simulate text with a 3D structure, more shadow parameter to make the shadow of the text more realistic, among others. 3) We compressed and saved the image in the JPEG format with different compression qualities to handle images of different quality. 4) A dilation mask of a text instance, including all its effects, was generated in the mask image to reduce the effect of JPEG artifacts around the text edge. Some samples of the generated image patches are shown in Fig. 5.

- **SCUT-Syn** [3] was created by Synthesis text engine [5], which contains 8,000 images for training and 800 images for testing. The background images of this dataset were collected from ICDAR 2013 [10] and ICDAR MLT-2017 [52], and the text instances in the background images were manually removed. Most test images were from the training set, and the training and testing sets were generated by sharing the same background images, although the synthesized text instances were different. We evaluated our method using only test images.

###### 2) Real-world Dataset:

- **ICDAR 2013** [10] is a widely used scene text images dataset that includes 229 training images and 223 testing images. All text instances are in English and are well focused. In this study, only the test set was used for the evaluation.
- **SCUT-EnsText** [4] is a comprehensive and challenge scene text removal dataset, containing 2,749 training images and 813 testing images, which are collected from ICDAR2013 [10], ICDAR-2015 [53], MS COCO-Text [54], SVT [55], MLT-2019 [56], and ArTs [23]. The text instances of this dataset are in Chinese or English with diverse shapes, such as horizontal text, arbitrary quadrilateral text, and curved text. All text instances were carefully erased by annotators with good visual quality. By providing original text annotation and text-erased ground-truth, this dataset can be comprehensively used for both qualitative and quantitative evaluation. In this

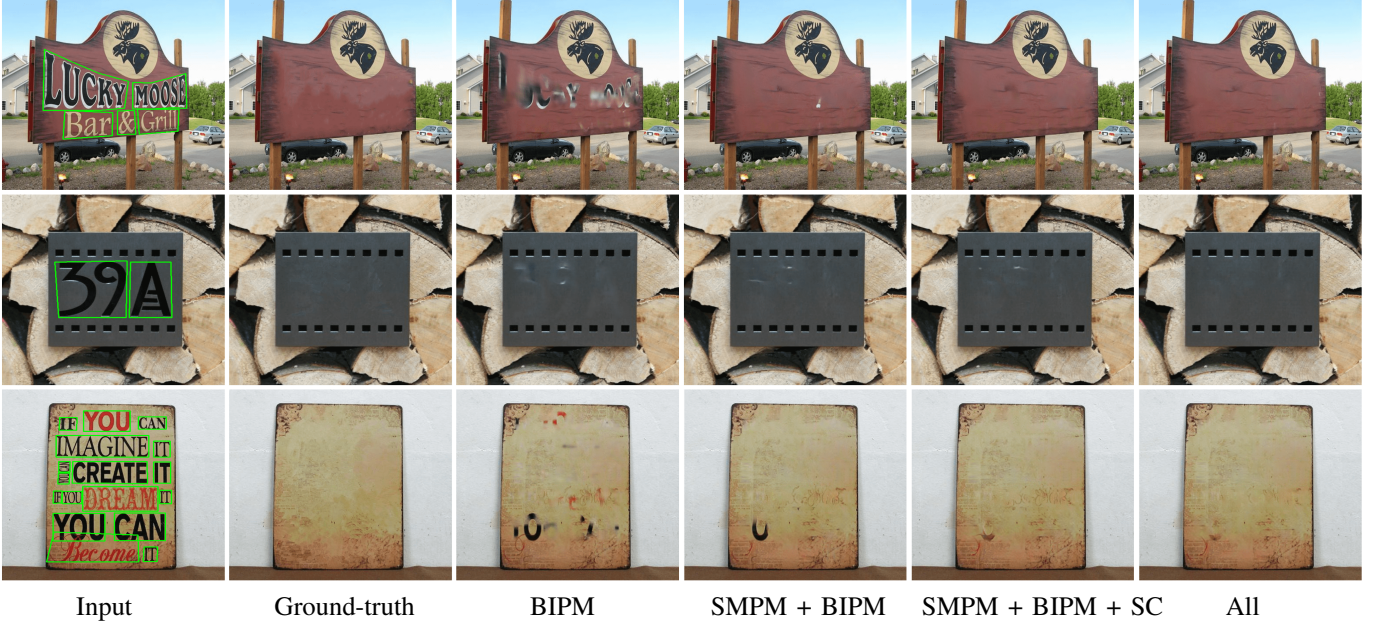


Fig. 6. Visual quality results of ablation study on SCUT-EnsText dataset. From left to right: input images, ground-truth, output of BIPM, output of SMPM+BIPM, output of SMPM+BIPM+SC, and output of all. SMPM: stroke mask prediction module. BIPM: background inpainting module. SC: Skip connection between two modules. SA: Self-attention block. All: SMPM + BIPM + SC + SA.

TABLE I  
ABLATION STUDY AND QUALITATIVE COMPARISON BETWEEN DIFFERENT CONFIGURATIONS OF OUR PROPOSED NETWORK ON SCUT-SYN AND SCUT-ENSTEXT DATASETS. SMPM: STROKE MASK PREDICTION MODULE. BIPM: BACKGROUND INPAINTING MODULE. SC: SKIP CONNECTION BETWEEN TWO MODULES. SA: SELF-ATTENTION BLOCK

Method	SCUT-Syn			SCUT-EnsText		
	PSNR↑	SSIM(%)↑	MSE↓	PSNR↑	SSIM(%)↑	MSE↓
BIPM (w/o partial conv)	34.78	96.67	0.00061	34.62	95.79	0.00114
SMPM + BIPM	37.74	97.31	0.00034	36.11	96.31	0.00077
SMPM + BIPM + SC	38.29	97.48	0.00030	36.36	96.39	0.00070
SMPM + BIPM + SC + SA (all)	<b>38.60</b>	<b>97.55</b>	<b>0.00024</b>	<b>37.08</b>	<b>96.54</b>	<b>0.00054</b>

study, we used the test set to evaluate the performance of our method.

### 3) Evaluation metrics:

- **Quantitative Evaluation** To quantitate the ability of a model on how much text can be erased, we follow [2]–[4], [7], [44] and utilize a baseline scene text detection model to detect texts in the text-erased images and evaluate how low are the precision, recall and F-score of the detection results. To make a fair comparison with previous studies, scene text detector EAST and ICDAR 2013 evaluation [22] protocols were used in the ICDAR 2013 dataset [10], text detector CRAFT [27], and ICDAR 2015 [53] protocols were adopted for the evaluation of SCUT-EnsText [4].
- **Qualitative Evaluation** We followed the previous image inpainting works by reporting metrics including peak signal-to-noise ratio (PSNR), the structural similarity index (SSIM) [57] and mean squared error (MSE). Higher SSIM, PSNR, and lower MSE values indicate better image restoration quality. Qualitative evaluations were conducted on both the SCUT-Syn [3] and SCUT-EnsText [4] datasets.

### C. Ablation Study

In this section, we investigate the effectiveness of the different settings of our proposed model. The stroke mask prediction module (SMPM), skip connection (SC) between two modules, and self-attention block (SA) are the focus. The qualitative evaluation results on the SCUT-Syn and SCUT-EnsText datasets are presented in Table I, and some text-erasing samples are shown in Fig. 6.

- **Stroke Mask Prediction Module** Stroke Mask Prediction Module aims to provide the pixel-level information of text region as the hole for Background Inpainting Module (BIPM), so that the network can learn more valid features from the non-text region and suppress the text residue. The qualitative results are presented in Table I. The text mask and partial convolutional layers can significantly improve the text erasing performance. It should be noted that without the mask image from the stroke mask prediction module, the partial convolutional layers in the background inpainting module will function as normal convolutional layers.
- **Skip Connection** Skip Connection linking and concatenating the low-resolution feature maps of two modules could provide the feature inside the text region for the decoder of background inpainting module, and improve



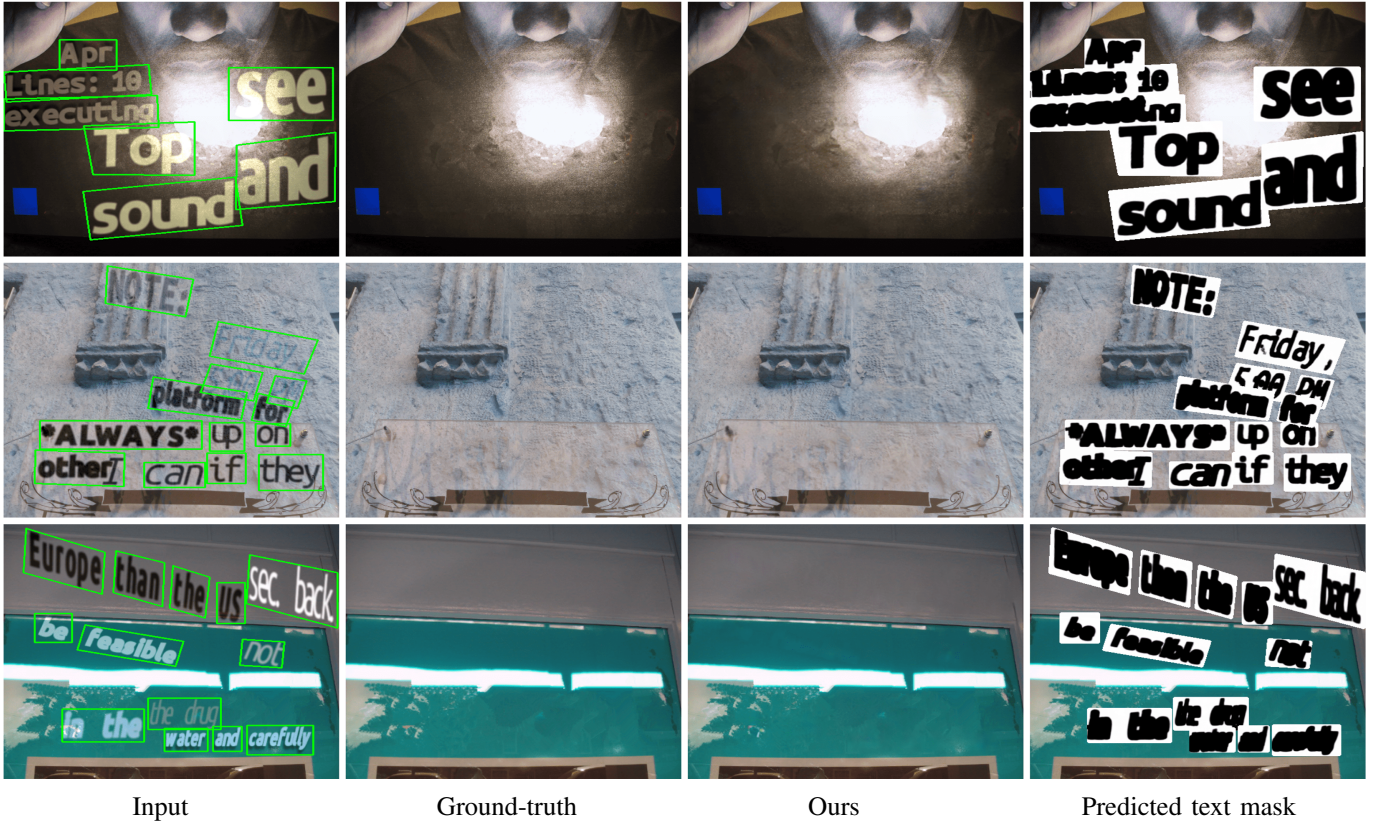


Fig. 7. Qualitative results of our method on the SCUT-Syn dataset. From left to right: input image and text bounding boxes, ground truth, our output, and predicted text mask.

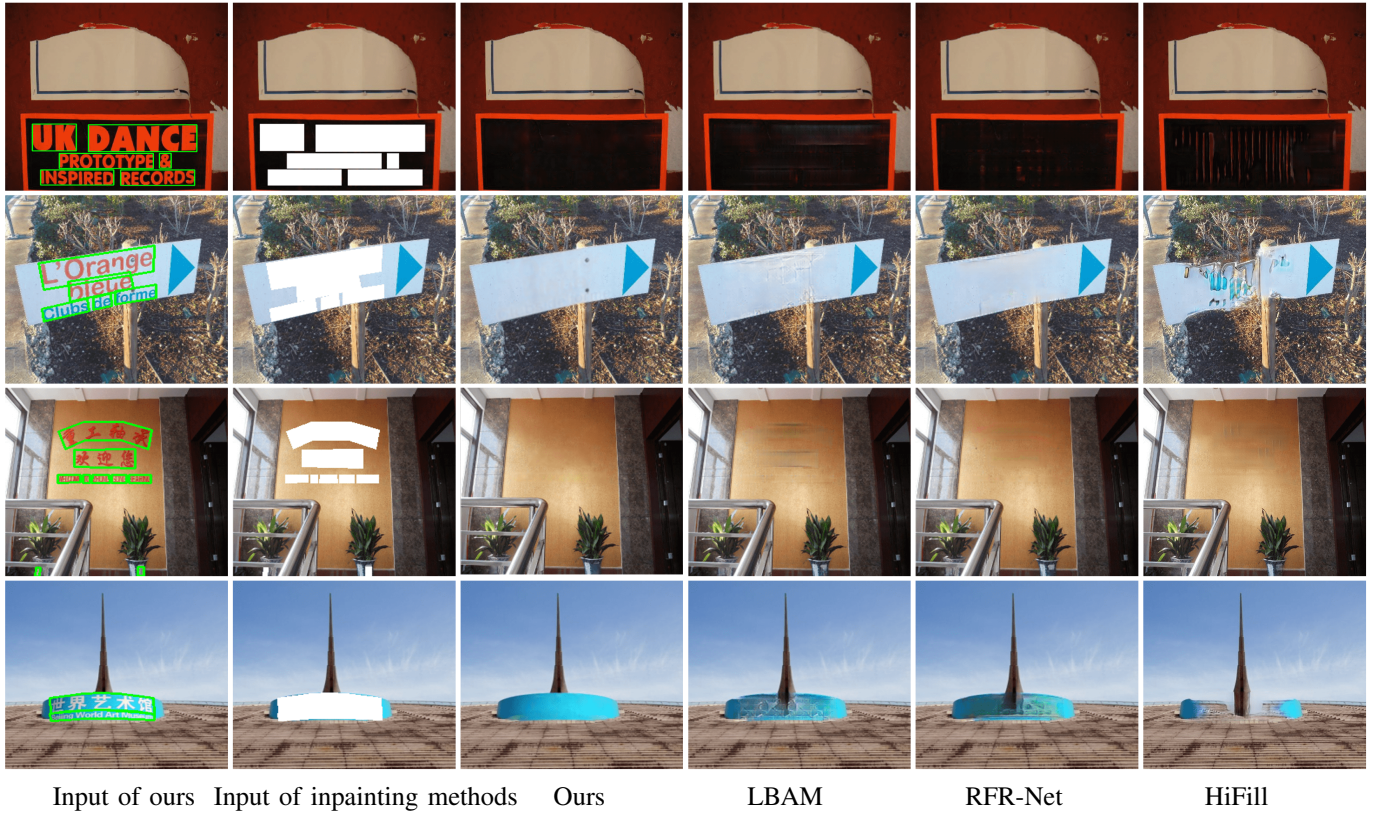
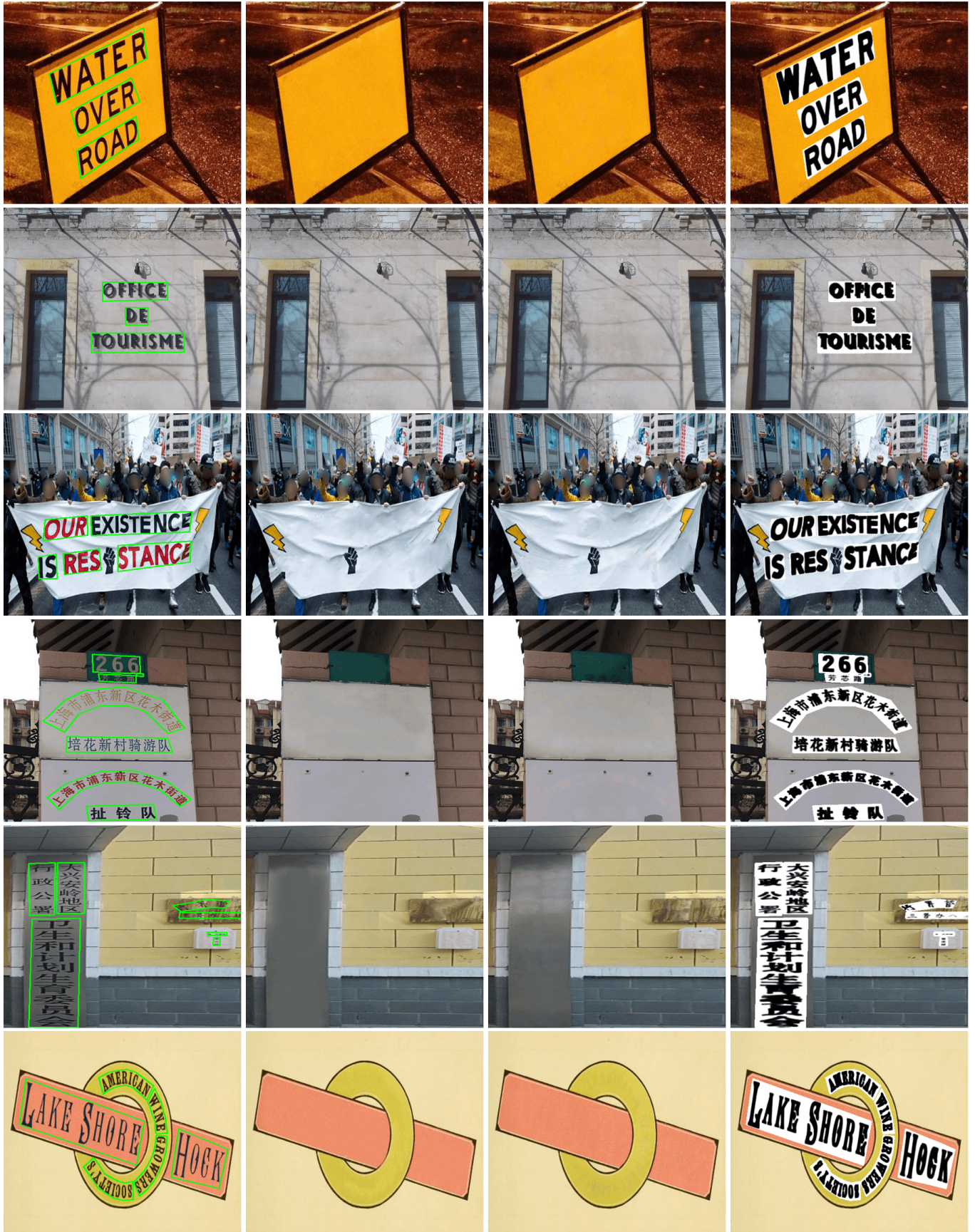


Fig. 8. Visual qualitative comparison between our method and state-of-the-art image inpainting methods on the SCUT-EnsText dataset. From left to right: input of our method, input of inpainting methods, output of our method, output of LBAM, output of RFR-Net, and output of HiFill.





Input

Ground-truth

Ours

Predicted text mask

Fig. 9. Qualitative results of our method on SCUT-EnsText dataset. From left to right: input, ground truth, output of our method, and predicted text mask.

TABLE II  
COMPARISON BETWEEN PREVIOUS SCENE TEXT-ERASING STUDIES AND OUR PROPOSED METHOD ON THE SCUT-SYN AND ICDAR2013 DATASETS.

Method	SCUT-Syn			ICDAR2013			Input
	PSNR $\uparrow$	SSIM( $\%$ ) $\uparrow$	MSE $\downarrow$	R $\downarrow$	P $\downarrow$	F $\downarrow$	
SceneTextEraser [1]	14.68	46.13	0.7148	10.08	39.09	16.03	Image
Pix2Pix [58]	25.60	89.86	0.2465	10.19	69.45	17.78	Image
EnsNet [3]	37.36	96.44	0.0021	5.66	73.42	10.51	Image
MTRNet [44]	29.71	94.43	0.01	0.18	16.67	0.36	Image (256 $\times$ 256) + Text Mask
Weak Supervision [7]	37.62	93.64	-	0.64	-	-	Image (256 $\times$ 256)
MTRNet++ [2]	34.55	<b>98.45</b>	0.0004	-	-	-	Image (256 $\times$ 256)
EraseNet [4]	38.32	97.67	<b>0.0002</b>	-	-	-	Image
Ours	<b>38.60</b>	97.55	<b>0.0002</b>	<b>0</b>	<b>0</b>	<b>0</b>	Image + BBox

TABLE III  
COMPARISON BETWEEN STATE-OF-THE-ART INPAINTING METHODS AND OUR PROPOSED METHOD ON THE SCUT-ENSTEXT DATASET.

Method	SCUT-EnsText			Input	Training dataset
	PSNR $\uparrow$	SSIM( $\%$ ) $\uparrow$	MSE $\downarrow$		
LBAM [36]	36.21	95.58	0.0007	Image (256 $\times$ 256) + Text Mask	Paris Street View [8]
RFR-Net [37]	36.95	96.12	0.0006	Image (256 $\times$ 256) + Text Mask	Paris Street View [8]
HiFill [38]	31.48	94.17	0.0021	Image + Text Mask	Places2 [59]
Ours	<b>37.89</b>	<b>97.02</b>	<b>0.0004</b>	Image (256 $\times$ 256) + BBox	Improved Synth text
Ours	<b>37.08</b>	<b>96.54</b>	<b>0.0005</b>	Image + BBox	Improved Synth text

TABLE IV  
COMPARISON BETWEEN STATE-OF-THE-ART SCENE TEXT-ERASING METHODS AND OUR PROPOSED METHOD ON THE SCUT-ENSTEXT DATASET.

Method	Qualitative eval			Quantitative eval			Input
	PSNR $\uparrow$	SSIM( $\%$ ) $\uparrow$	MSE $\downarrow$	R $\downarrow$	P $\downarrow$	F $\downarrow$	
Original images	-	-	-	69.5	79.7	74.3	-
SceneTextEraser [4]	25.47	90.14	0.0047	5.9	40.9	10.2	Image
EnsNet [3]	29.54	92.74	0.0024	32.8	68.7	44.4	Image
EraseNet [4]	32.30	95.42	0.0015	4.6	53.2	8.5	Image
Detector [27] + Ours	<b>35.34</b>	<b>96.24</b>	<b>0.0009</b>	<b>0.035</b>	<b>0.443</b>	<b>0.065</b>	Image

the accuracy and stability of text mask prediction. Table I implies that the skip connection between the two modules could improve the erasing quality of the image in both the SCUT-Syn and SCUT-EnsText datasets.

- **Self-Attention Block** To confirm the importance of self-attention block, we trained our network without the SA block. From Table I, we can see that the performance of our network decreases when the self-attention block is missing.

#### D. Comparison With State-of-the-Art Methods

To evaluate the performance of our proposed method, we compared it with recent state-of-the-art methods on the SCUT-Syn, ICDAR2013, and SCUT-EnsText datasets. For the SCUT-Syn and ICDAR2013 datasets, the results of SceneTextEraser, Pix2Pix, and EnsNet were implemented and reported by Zhang *et al.* [3]. The results of MTRNet [44], Weak Supervision [7], MTRNet++ [2], and EraseNet [4] were collected from official reports of papers. If there is no special description, the resolution of the input image is  $512 \times 512$ . Table II shows the results for the SCUT-Syn [3] and ICDAR2013 [10] datasets. Our proposed method achieves the highest PSNR in the SCUT-Syn dataset and the lowest recall, precision, and F-score in the ICDAR2013 dataset when the bounding boxes are provided. Some text erasing examples on the SCUT-Syn dataset are shown in Fig. 7. We consider the reason why MTRNet++ and EraseNet could generate higher SSIM images on the

SCUT-Syn dataset is because most test images are included in the training set and share the same background images with training images when they are generated. We did not train our model using the SCUT-Syn training set, thereby causing a lower SSIM in our results. We believe that this dataset cannot fully reflect the generalization ability of a network when it is used for training. R, P, and F represent recall, precision, and F-score, respectively, which are the detection results of EAST under the ICDAR2013 evaluation protocol.

For the SCUT-EnsText dataset, we compared our method with state-of-the-art image inpainting methods and scene text erasing methods. The comparison results with the inpainting methods of the SCUT-EnsText dataset are shown in Table III. Our scene text erasing method achieves a superb result in image quality when the text bounding box information is provided. We made some revisions to the original text location annotation since we observed some unmatched cases between the location of the erased text and the text bounding box of the ground truth. We selected three state-of-the-art image inpainting methods: LBAM [36], RFR-Net [37] and HiFill [38]. The LBAM [36] and RFR-Net [37] models were pretrained on the Paris Street View dataset [8], and HiFill [38] model was pretrained on the Places2 dataset [59]. For a fair comparison with the pretrained inpainting methods, we generated the hole mask directly from our revised bounding box and resized the input images to the same size because some pretrained inpainting models only work at a resolution of  $256 \times 256$ . Our method can generate higher quality images



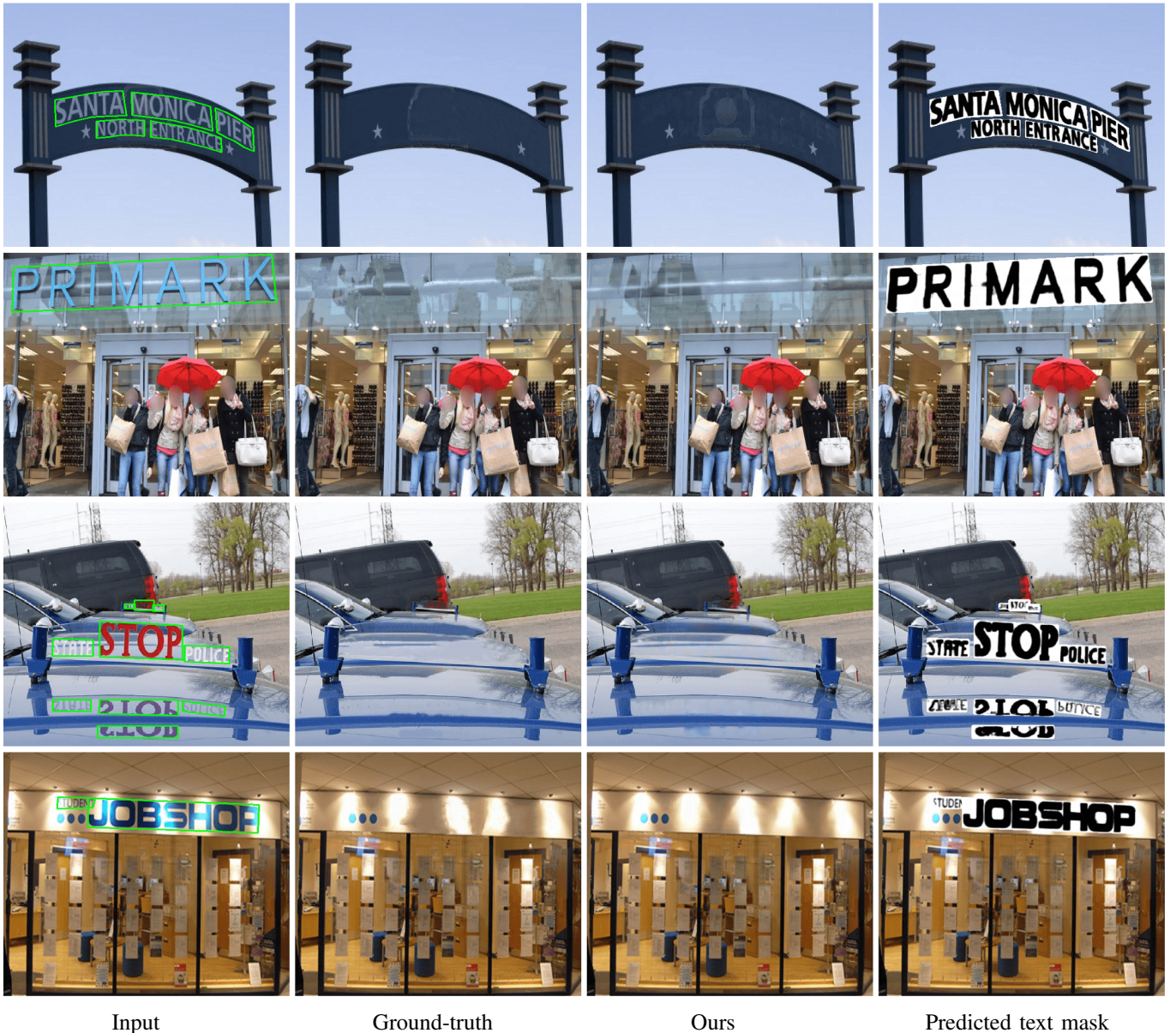


Fig. 10. Our method is able to retain more detailed background information and restore the background texture. From left to right: input image and text bounding boxes, ground truth, our output, and predicted text mask.

than using state-of-the-art image inpainting methods under the same conditions. Some visual quality comparison samples are presented in Fig. 8. We observed that there are always some strange textures or artifacts in the text-erased images inpainted by pretrained image inpainting methods, causing unnatural erasing results. We also found that the inpainting logic of HiFill [38] prefers to restore the hole region with further background information, leading to worse results than the other two methods. As this model is pretrained on the Places2 [59] dataset, although it contains many indoor and urban views, this pretrained model shows a serious domain shift problem when facing scene text erasing tasks.

In addition, we use our method with a scene text detector as a two-step automatic scene text eraser. In our experiment, we used CRAFT [27] for scene text detection and produced arbitrary quadrilateral bounding boxes as the input for our

method. We compared our proposed methods with previous scene text erasing methods on the SCUT-EnsText dataset. The results are shown in Table IV, implying that the first detection and inpainting by our method also significantly outperforms existing state-of-the-art methods in both qualitative and quantitative evaluations. Here R, P, and F denote recall, precision, and F-score, respectively, which are the detection results of the CRAFT [27] under the ICDAR2015 evaluation [53] protocol. Some qualitative results of our method on the SCUT-EnsText dataset are shown in Fig. 9. Our method could clearly remove the text region, regardless of whether the text instances were of various shapes, fonts, and illumination conditions.

#### E. Discussion

From the experimental results, we observed that the model trained by our improved synthetic text dataset has different



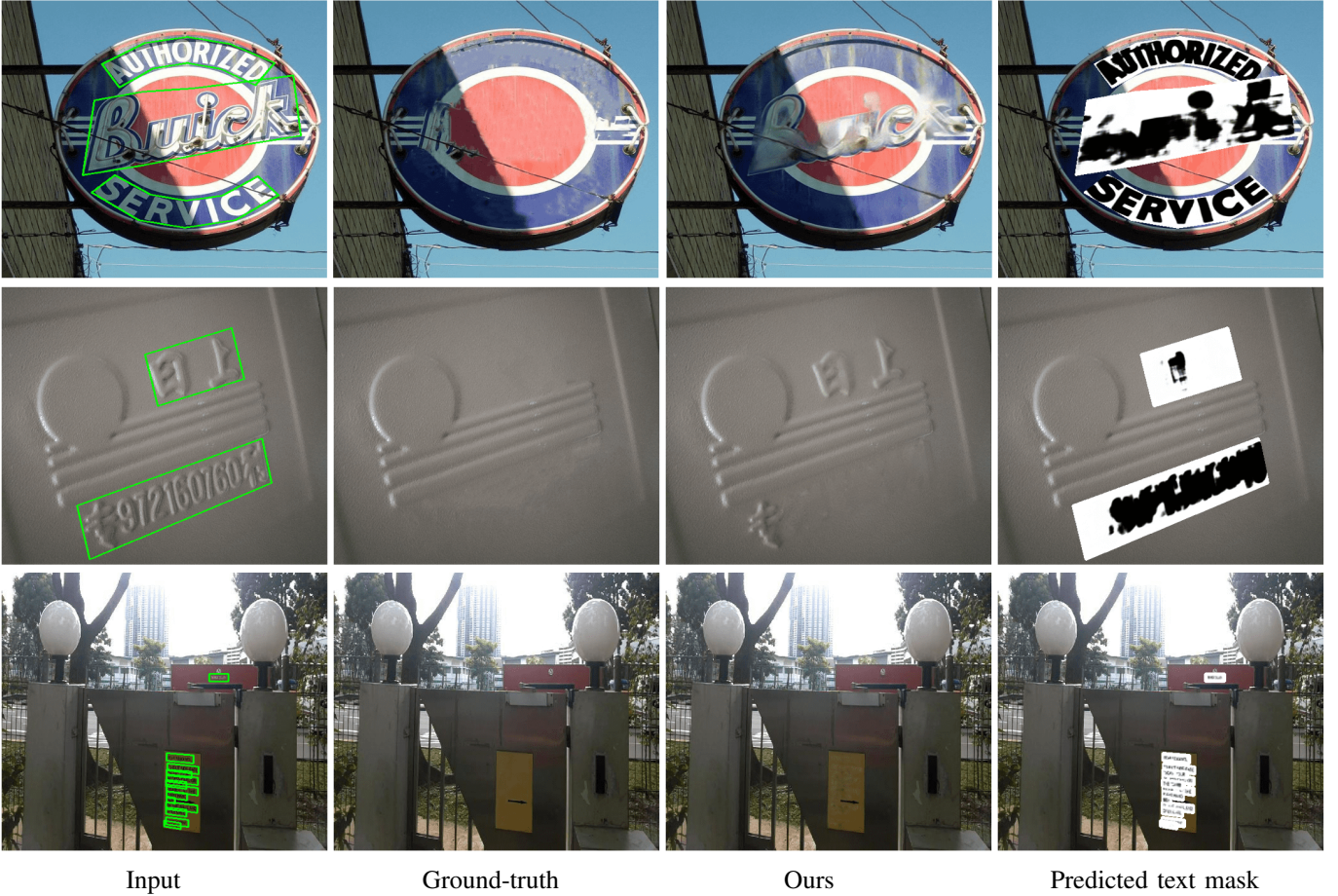


Fig. 11. Some failure cases of our method. From left to right: input image and text bounding boxes, ground truth, our output, and predicted text mask.

inpainting logic from the annotations of the real-world scene-text removal dataset, which was manually edited by using Photoshop. As shown in Fig. 10, we observed that our method can erase the text while retaining more detailed background information of the image. Moreover, benefiting from the model design and a large amount of training data, our method could reconstruct some background textures for better visual perception. On the contrary, due to the limited text style of the synthetic text engine, our method makes failure text erasing when facing the text in a special shape or stereoscopic text under complicated illumination conditions as depicted in Fig. 11. Because we propose to erase the text at the image patch level, our method encounters some difficulty in solving small text instances in the images. As there are always JPEG boundary artifacts surrounding the text edge, our model could hardly discriminate whether the pixel near the text edge belongs to the background or the artifact, borrowing the features from artifact regions will result in the text region being inpainted by strange colors, causing bad inpainting results.

## V. CONCLUSION

In this study, we proposed a novel scene text erasing method that addresses the weak text location problem of one-step methods and the domain shift problem of pretrained inpainting models trained on street view or Places datasets. Our model is trained using only our improved synthetic text dataset. It works

on the image patch level and inpaints the text region based on a predicted text stroke mask, which can preserve more background information. By employing a stroke mask prediction module, partial convolution layers, an attention block in the background inpainting module, and skip connection between two modules, our method could reasonably erase scene text with texture restoration. Using a pretrained scene text detector to provide text location information for our model, it can function as an end-to-end scene text eraser to automatically remove text in the wild. Our experimental results show that it achieves a better performance than existing state-of-the-art methods.

## REFERENCES

- [1] T. Nakamura, A. Zhu, K. Yanai, and S. Uchida, "Scene Text Eraser," in *Proceedings of the International Conference on Document Analysis and Recognition, ICDAR*, 2017.
- [2] O. Tursun, S. Denman, R. Zeng, S. Sivapalan, S. Sridharan, and C. Fookes, "MTRNet++: One-stage mask-based scene text eraser," *Computer Vision and Image Understanding*, 2020.
- [3] S. Zhang, Y. Liu, L. Jin, Y. Huang, and S. Lai, "EnsNet: Ensconce text in the wild," in *33rd AAAI Conference on Artificial Intelligence, AAAI 2019, 31st Innovative Applications of Artificial Intelligence Conference, IAAI 2019 and the 9th AAAI Symposium on Educational Advances in Artificial Intelligence, EAAI 2019*, 2019.
- [4] C. Liu, Y. Liu, L. Jin, S. Zhang, C. Luo, and Y. Wang, "EraseNet: End-to-End Text Removal in the Wild," *IEEE Transactions on Image Processing*, vol. 29, pp. 8760–8775, 2020.

- [5] A. Gupta, A. Vedaldi, and A. Zisserman, "Synthetic Data for Text Localisation in Natural Images," in *2016 IEEE Conference on Computer Vision and Pattern Recognition (CVPR)*, Jun. 2016, pp. 2315–2324.
- [6] X. Bian, C. Wang, W. Quan, J. Ye, X. Zhang, and D. M. Yan, "Scene text removal via cascaded text stroke detection and erasing," *arXiv*, pp. 1–14, 2020.
- [7] J. Zdenek and H. Nakayama, "Erasing Scene Text with Weak Supervision," in *2020 IEEE Winter Conference on Applications of Computer Vision (WACV)*, Mar. 2020, pp. 2227–2235.
- [8] D. Pathak, P. Krahenbuhl, J. Donahue, T. Darrell, and A. A. Efros, "Context Encoders: Feature Learning by Inpainting," in *2016 IEEE Conference on Computer Vision and Pattern Recognition (CVPR)*, Jun. 2016, pp. 2536–2544.
- [9] O. Russakovsky, J. Deng, H. Su, J. Krause, S. Satheesh, S. Ma, Z. Huang, A. Karpathy, A. Khosla, M. Bernstein, A. C. Berg, and L. Fei-Fei, "ImageNet Large Scale Visual Recognition Challenge," *International Journal of Computer Vision*, vol. 115, no. 3, pp. 211–252, Dec. 2015.
- [10] D. Karatzas, F. Shafait, S. Uchida, M. Iwamura, L. G. I. Bigorda, S. R. Mestre, J. Mas, D. F. Mota, J. A. Almazan, and L. P. De Las Heras, "ICDAR 2013 robust reading competition," in *Proceedings of the International Conference on Document Analysis and Recognition, ICDAR, 2013*.
- [11] Xiangrong Chen and A. Yuille, "Detecting and reading text in natural scenes," in *Proceedings of the 2004 IEEE Computer Society Conference on Computer Vision and Pattern Recognition, 2004. CVPR 2004.*, vol. 2, 2004, pp. 366–373.
- [12] L. Neumann and J. Matas, "A Method for Text Localization and Recognition in Real-World Images," in *Computer Vision – ACCV 2010*, 2011, vol. 6494, pp. 770–783.
- [13] A. Jamil, I. Siddiqi, F. Arif, and A. Raza, "Edge-Based Features for Localization of Artificial Urdu Text in Video Images," in *2011 International Conference on Document Analysis and Recognition*, Sep. 2011, pp. 1120–1124.
- [14] A. Mosleh, N. Bouguila, and A. B. Hamza, "Image Text Detection Using a Bandlet-Based Edge Detector and Stroke Width Transform," in *Proceedings of the British Machine Vision Conference 2012*, 2012, pp. 63.1–63.12.
- [15] W. Huang, Z. Lin, J. Yang, and J. Wang, "Text Localization in Natural Images Using Stroke Feature Transform and Text Covariance Descriptors," in *2013 IEEE International Conference on Computer Vision*, Dec. 2013, pp. 1241–1248.
- [16] M. Liao, B. Shi, X. Bai, X. Wang, and W. Liu, "TextBoxes: A Fast Text Detector with a Single Deep Neural Network," *Thirty-First AAAI Conference on Artificial Intelligence*, vol. 31, p. 7, 2017.
- [17] W. Liu, D. Anguelov, D. Erhan, C. Szegedy, S. Reed, C.-Y. Fu, and A. C. Berg, "SSD: Single Shot MultiBox Detector," in *Computer Vision – ECCV 2016*, 2016, vol. 9905, pp. 21–37.
- [18] Z. Tian, W. Huang, T. He, P. He, and Y. Qiao, "Detecting Text in Natural Image with Connectionist Text Proposal Network," in *Computer Vision – ECCV 2016*, 2016, vol. 9912, pp. 56–72.
- [19] S. Ren, K. He, R. Girshick, and J. Sun, "Faster R-CNN: Towards Real-Time Object Detection with Region Proposal Networks," *IEEE Transactions on Pattern Analysis and Machine Intelligence*, vol. 39, no. 6, pp. 1137–1149, Jun. 2017.
- [20] J. Ma, W. Shao, H. Ye, L. Wang, H. Wang, Y. Zheng, and X. Xue, "Arbitrary-Oriented Scene Text Detection via Rotation Proposals," *IEEE Transactions on Multimedia*, vol. 20, no. 11, pp. 3111–3122, Nov. 2018.
- [21] B. Shi, X. Bai, and S. Belongie, "Detecting Oriented Text in Natural Images by Linking Segments," in *2017 IEEE Conference on Computer Vision and Pattern Recognition (CVPR)*, Jul. 2017, pp. 3482–3490.
- [22] X. Zhou, C. Yao, H. Wen, Y. Wang, S. Zhou, W. He, and J. Liang, "EAST: An Efficient and Accurate Scene Text Detector," in *2017 IEEE Conference on Computer Vision and Pattern Recognition (CVPR)*, Jul. 2017, pp. 2642–2651.
- [23] C. K. Chng, E. Ding, J. Liu, D. Karatzas, C. S. Chan, L. Jin, Y. Liu, Y. Sun, C. C. Ng, C. Luo, Z. Ni, C. M. Fang, S. Zhang, and J. Han, "ICDAR2019 robust reading challenge on arbitrary-shaped text-RRCArT," in *Proceedings of the International Conference on Document Analysis and Recognition, ICDAR, 2019*.
- [24] P. Lyu, M. Liao, C. Yao, W. Wu, and X. Bai, "Mask TextSpotter: An End-to-End Trainable Neural Network for Spotting Text with Arbitrary Shapes," in *Computer Vision – ECCV 2018*, 2018, vol. 11218, pp. 71–88.
- [25] K. He, G. Gkioxari, P. Dollar, and R. Girshick, "Mask R-CNN," in *2017 IEEE International Conference on Computer Vision (ICCV)*, Oct. 2017, pp. 2980–2988.
- [26] S. Long, J. Ruan, W. Zhang, X. He, W. Wu, and C. Yao, "TextSnake: A Flexible Representation for Detecting Text of Arbitrary Shapes," in *Computer Vision – ECCV 2018*, 2018, vol. 11206, pp. 19–35.
- [27] Y. Baek, B. Lee, D. Han, S. Yun, and H. Lee, "Character Region Awareness for Text Detection," in *2019 IEEE/CVF Conference on Computer Vision and Pattern Recognition (CVPR)*, Jun. 2019, pp. 9357–9366.
- [28] Y. Li, Z. Wu, S. Zhao, X. Wu, Y. Kuang, Y. Yan, S. Ge, K. Wang, W. Fan, X. Chen, and Y. Wang, "PSENet: Psoriasis Severity Evaluation Network," *Proceedings of the AAAI Conference on Artificial Intelligence*, vol. 34, no. 01, pp. 800–807, Apr. 2020.
- [29] A. A. Efros and W. T. Freeman, "Image quilting for texture synthesis and transfer," in *Proceedings of the 28th Annual Conference on Computer Graphics and Interactive Techniques - SIGGRAPH '01*, 2001, pp. 341–346.
- [30] C. Barnes, E. Shechtman, A. Finkelstein, and D. B. Goldman, "Patch-Match: A randomized correspondence algorithm for structural image editing," *ACM Transactions on Graphics*, vol. 28, no. 3, pp. 1–11, Jul. 2009.
- [31] Zongben Xu and Jian Sun, "Image Inpainting by Patch Propagation Using Patch Sparsity," *IEEE Transactions on Image Processing*, vol. 19, no. 5, pp. 1153–1165, May 2010.
- [32] S. Darabi, E. Shechtman, C. Barnes, D. B. Goldman, and P. Sen, "Image melding: Combining inconsistent images using patch-based synthesis," *ACM Transactions on Graphics*, vol. 31, no. 4, pp. 1–10, Aug. 2012.
- [33] S. Iizuka, E. Simo-Serra, and H. Ishikawa, "Globally and locally consistent image completion," *ACM Transactions on Graphics*, vol. 36, no. 4, pp. 1–14, Jul. 2017.
- [34] G. Liu, F. A. Reda, K. J. Shih, T.-C. Wang, A. Tao, and B. Catanzaro, "Image Inpainting for Irregular Holes Using Partial Convolutions," in *Computer Vision – ECCV 2018*, 2018, vol. 11215, pp. 89–105.
- [35] J. Yu, Z. Lin, J. Yang, X. Shen, X. Lu, and T. Huang, "Free-Form Image Inpainting With Gated Convolution," in *2019 IEEE/CVF International Conference on Computer Vision (ICCV)*, Oct. 2019, pp. 4470–4479.
- [36] C. Xie, S. Liu, C. Li, M.-M. Cheng, W. Zuo, X. Liu, S. Wen, and E. Ding, "Image Inpainting With Learnable Bidirectional Attention Maps," in *2019 IEEE/CVF International Conference on Computer Vision (ICCV)*, Oct. 2019, pp. 8857–8866.
- [37] J. Li, N. Wang, L. Zhang, B. Du, and D. Tao, "Recurrent Feature Reasoning for Image Inpainting," in *2020 IEEE/CVF Conference on Computer Vision and Pattern Recognition (CVPR)*, Jun. 2020, pp. 7757–7765.
- [38] Z. Yi, Q. Tang, S. Azizi, D. Jang, and Z. Xu, "Contextual Residual Aggregation for Ultra High-Resolution Image Inpainting," in *2020 IEEE/CVF Conference on Computer Vision and Pattern Recognition (CVPR)*, Jun. 2020, pp. 7505–7514.
- [39] C. W. Lee, K. Jung, and H. J. Kim, "Automatic text detection and removal in video sequences," *Pattern Recognition Letters*, vol. 24, no. 15, pp. 2607–2623, 2003.
- [40] E. A. Pneumatikakis and P. Maragos, "An inpainting system for automatic image structure - texture restoration with text removal," in *2008 15th IEEE International Conference on Image Processing*, 2008, pp. 2616–2619.
- [41] A. Mosleh, N. Bouguila, and A. B. Hamza, "Automatic Inpainting Scheme for Video Text Detection and Removal," *IEEE Transactions on Image Processing*, vol. 22, no. 11, pp. 4460–4472, Nov. 2013.
- [42] M. Khodadadi and A. Behrad, "Text localization, extraction and inpainting in color images," *ICEE 2012 - 20th Iranian Conference on Electrical Engineering*, pp. 1035–1040, 2012.
- [43] P. D. Wagh and D. R. Patil, "Text detection and removal from image using inpainting with smoothing," *2015 International Conference on Pervasive Computing: Advance Communication Technology and Application for Society, ICPC 2015*, vol. 00, no. c, pp. 1–4, 2015.
- [44] O. Tursun, R. Zeng, S. Denman, S. Sivapalan, S. Sridharan, and C. Fookes, "MTRNet: A generic scene text eraser," in *Proceedings of the International Conference on Document Analysis and Recognition, ICDAR, 2019*.
- [45] C. Zheng, T.-J. Cham, and J. Cai, "Pluralistic Image Completion," in *2019 IEEE/CVF Conference on Computer Vision and Pattern Recognition (CVPR)*, Jun. 2019, pp. 1438–1447.
- [46] K. He, X. Zhang, S. Ren, and J. Sun, "Deep Residual Learning for Image Recognition," in *2016 IEEE Conference on Computer Vision and Pattern Recognition (CVPR)*, Jun. 2016, pp. 770–778.
- [47] F. Milletari, N. Navab, and S. A. Ahmadi, "V-Net: Fully convolutional neural networks for volumetric medical image segmentation," in *Proceedings - 2016 4th International Conference on 3D Vision, 3DV 2016*, 2016.

- [48] Y. Cao, J. Xu, S. Lin, F. Wei, and H. Hu, "GCNet: Non-Local Networks Meet Squeeze-Excitation Networks and Beyond," in *2019 IEEE/CVF International Conference on Computer Vision Workshop (ICCVW)*, Oct. 2019, pp. 1971–1980.
- [49] L. A. Gatys, A. S. Ecker, and M. Bethge, "Image Style Transfer Using Convolutional Neural Networks," in *Proceedings of the IEEE Computer Society Conference on Computer Vision and Pattern Recognition*, vol. 2016-Decem, 2016.
- [50] J. Johnson, A. Alahi, and L. Fei-Fei, "Perceptual Losses for Real-Time Style Transfer and Super-Resolution," in *Computer Vision – ECCV 2016*, 2016, vol. 9906, pp. 694–711.
- [51] D. P. Kingma and J. L. Ba, "Adam: A method for stochastic optimization," in *3rd International Conference on Learning Representations, ICLR 2015 - Conference Track Proceedings*, 2015.
- [52] N. Nayef, F. Yin, I. Bizid, H. Choi, Y. Feng, D. Karatzas, Z. Luo, U. Pal, C. Rigaud, J. Chazalon, W. Khelif, M. M. Luqman, J. C. Burie, C. L. Liu, and J. M. Ogier, "ICDAR2017 Robust Reading Challenge on Multi-Lingual Scene Text Detection and Script Identification - RRC-MLT," in *Proceedings of the International Conference on Document Analysis and Recognition, ICDAR*, 2017.
- [53] D. Karatzas, L. Gomez-Bigorda, A. Nicolaou, S. Ghosh, A. Bagdanov, M. Iwamura, J. Matas, L. Neumann, V. R. Chandrasekhar, S. Lu, F. Shafait, S. Uchida, and E. Valveny, "ICDAR 2015 competition on Robust Reading," in *Proceedings of the International Conference on Document Analysis and Recognition, ICDAR*, 2015.
- [54] A. Veit, T. Matera, L. Neumann, J. Matas, and S. Belongie, "COCO-Text: Dataset and Benchmark for Text Detection and Recognition in Natural Images," *arXiv:1601.07140 [cs]*, Jun. 2016.
- [55] K. Wang and S. Belongie, "Word Spotting in the Wild," in *Computer Vision – ECCV 2010*, 2010, vol. 6311, pp. 591–604.
- [56] N. Nayef, C. L. Liu, J. M. Ogier, Y. Patel, M. Busta, P. N. Chowdhury, D. Karatzas, W. Khelif, J. Matas, U. Pal, and J. C. Burie, "ICDAR2019 robust reading challenge on multi-lingual scene text detection and recognition-RRC-MLT-2019," in *Proceedings of the International Conference on Document Analysis and Recognition, ICDAR*, 2019.
- [57] Z. Wang, A. C. Bovik, H. R. Sheikh, and E. P. Simoncelli, "Image quality assessment: From error visibility to structural similarity," *IEEE Transactions on Image Processing*, 2004.
- [58] P. Isola, J.-Y. Zhu, T. Zhou, and A. A. Efros, "Image-to-Image Translation with Conditional Adversarial Networks," in *2017 IEEE Conference on Computer Vision and Pattern Recognition (CVPR)*, Jul. 2017, pp. 5967–5976.
- [59] B. Zhou, A. Lapedriza, A. Khosla, A. Oliva, and A. Torralba, "Places: A 10 Million Image Database for Scene Recognition," *IEEE Transactions on Pattern Analysis and Machine Intelligence*, vol. 40, no. 6, pp. 1452–1464, Jun. 2018.



**Yoshihiro Sugaya** (Member, IEEE) received his B.E., M.E., and Ph.D. degrees from Tohoku University, Sendai, Japan in 1995, 1997, and 2002, respectively. He is currently an associate professor at the Graduate School of Engineering, Tohoku University. His research interests include computer vision, pattern recognition, image processing, parallel processing, and distributed computing. Dr. Sugaya is a member of the Institute of Electronics, Information and Communication Engineers (IEICE) and the Information Processing Society of Japan.



**Shinichiro Omachi** (M'96-SM'11) received his B.E., M.E., and Ph.D. degrees in Information Engineering from Tohoku University, Japan, in 1988, 1990, and 1993, respectively. He worked as an assistant professor at the Education Center for Information Processing at Tohoku University from 1993 to 1996. Since 1996, he has been with the Graduate School of Engineering at Tohoku University, where he is currently a professor. From 2000 to 2001, he was a visiting associate professor at Brown University. His research interests include pattern recognition, computer vision, image processing, image coding, and parallel processing. He served as the Editor-in-Chief of IEICE Transactions on Information and Systems from 2013 to 2015. Dr. Omachi is a member of the Institute of Electronics, Information and Communication Engineers, the Information Processing Society of Japan, among others. He received the IAPR/ICDAR Best Paper Award in 2007, the Best Paper Method Award of the 33rd Annual Conference of the GfKI in 2010, the ICFHR Best Paper Award in 2010, and the IEICE Best Paper Award in 2012. He is currently the Vice Chair of the IEEE Sendai Section.



**Zhengmi Tang** received his B.E. degree from Xidian University, Shaanxi, China, in 2017 and his M.E. degree in cybernetics engineering from Hiroshima University, Hiroshima, Japan, in 2020. He is currently pursuing a Ph.D. degree in communication engineering in the iic-lab at Tohoku University, Japan. His current research interests include computer vision, scene text detection, and data synthesis.



**Tomo Miyazaki** (Member, IEEE) received his B.E. and Ph.D. degrees from Yamagata University (2006) and Tohoku University (2011), respectively. From 2011 to 2012, he worked on the geographic information system at Hitachi, Ltd. From 2013 to 2014, he worked at Tohoku University as a post-doctoral researcher. Since 2015, he has been an assistant professor. His research interests include pattern recognition and image processing.